Global fish abundance estimation from regular sampling: the geostatistical transitive method

Nicolas Bez

Abstract: This article deals with the estimation of fish biomass based on regular samplings. The geostatistical transitive method is a design-based spatially explicit method based on few and falsifiable assumptions concerning the sampling strategy. The falsifiability of a hypothesis corresponds to our capacity to control its adequacy to field data in practice. We first describe the basics of the method, mention the questions relative to the covariogram estimation, the units, and the projections of the coordinates, and explain how to fit the model to the experimental covariogram. We then apply the method to an ICES (International Council for the Exploration of the Sea) triennial mackerel egg survey, with regular sampling, and to a Moroccan octopus survey, with regular stratified sampling. To compare the present technique with existing methods, the number and the falsifiability of their respective hypotheses are considered in addition to the bias, the convergence, and the estimation variance. As is often the case, data are assumed to be synoptic, and we discuss two examples of spatiotemporal methods.

Résumé : Cet article aborde la question de l'estimation de l'abondance globale d'une population à partir d'un échantillonnage régulier. La méthode géostatistique transitive est une méthode spatiale compatible avec de tels échantillonnages. Elle est basée sur un petit nombre d'hypothèses falsifiables (réfutables) qui portent sur la stratégie d'échantillonnage. On commence par rappeller les fondements théoriques de cette méthode, présenter les problèmes pratiques concernant l'estimation du covariogramme, le choix des unités et la projection des coordonnées et par donner des indications sur l'inférence des modèles. La méthode est ensuite appliquée à une campagne triennale CIEM d'estimations des œufs de maquereau basée sur un échantillonnage régulier et à une campagne marocaine d'évaluation du poulpe qui reposent sur un échantillonnage stratifié aléatoire. Afin de comparer l'approche transitive à d'autres méthodes existantes, le nombre et la falsifiabilité des hypothèses mises en jeux dans chacune des méthodes évoquées sont discutées en plus des propriétés de non biais, de convergence et de variance d'estimation. Comme souvent, l'approche transitive suppose que les données ont été récoltées en même temps. Ceci amène à mentionner deux exemples d'approches spatio-temporelles.

Introduction

The assessment of fish populations by direct observation should be based ideally on data that are precise (no measurement error), synoptic, global (cover the entire population area), and as exhaustive as possible (spatially complete). However, it is not possible to fulfill these requirements in practice and compromises have to be made between the size of the gear, the number of samples, their location, the time needed to visit all sample locations, and the overall time granted for the survey. In addition, surveys often share several objectives targeting several species in a single survey or looking for environmental information to interpret stock dynamics, which leads to more compromises when defining the sampling strategies. A general rule is that a regular sampling design allows for an optimal balance between the different objectives of a survey (Simmonds and Fryer 1996). Contrary to random samplings that allow for direct estimations through design-based approaches (e.g., Cochran 1977), the use of spatially regular samplings requires a model of spatial covariance (model-based approaches) to generate an estimation variance.

When geostatistics is applied, it is often done in the so-called intrinsic approach using variograms (Rivoirard et al. 2000; Petitgas 2001). However, the estimation of the variogram is often difficult in practice because of the characteristics of the fish data (i.e., the location of the high values in the field, the numerous low or zero densities) and because of the hypotheses associated with the use of the variogram (Matheron 1971; Petitgas 1993; Bez and Rivoirard 2001). Although some authors are suggesting more robust estimators for the variogram (Cressie 1991), the method itself might be regarded as based on too strong hypotheses. In this regard, one usually looks for estimations based on as few hypotheses as possible (principle of parsimony) as this reduces the possibilities to observe discrepancies between the characteristics of the data and the assumptions on which the estimator is based (robustness).

To estimate global estimation variance in the case of regular sampling, Matheron (1971) developed the transitive approach, a model-based method that requires fewer hypotheses than the intrinsic one. Despite its simplicity, the use of the transitive approach has not been widespread in the fisheries community and is only mentioned in short sections in the fisheries literature. Petitgas (1993) used it in one dimension

Received 18 December 2001. Accepted 15 November 2002. Published on the NRC Research Press Web site at http://cjfas.nrc.ca on 10 January 2003.
J16669

N. Bez. Centre de Géostatistique, 35 rue Saint Honoré, 77305 Fontainebleau, France (e-mail: bez@cg.ensmp.fr).

 DOI: 10.1139/F02-155

for the very special case of acoustic surveys with parallel and equidistant transects. Working in two dimensions on mackerel eggs and larvae, Gohin used it to compute a global estimation variance of the number of eggs but did not publish it (F. Gohin, IFREMER, 29280 Plouzané, France, personal communication). However, this method has recently been shown to be appropriate for the treatment of spatial data sets with numerous zeroes (Bez and Rivoirard 2001) as all samples, including the zero data, are considered. It has also been shown to be appropriate for global estimation variance in random stratified samplings (Bez et al. 1995). Our objective here is to present in detail the theory and the practical implementation of the transitive approach.

The first part of this paper is devoted to the presentation of the method. The second part examines two typical situations: a regular grid design used in ICES (International Council for the Exploration of the Sea) triennial egg surveys and a random stratified design in which samples are located at random and independent from one another in each cell of a regular grid used in Moroccan surveys.

Methods

Theory

Regionalized variable covariogram and relative covariogram

Let x represent a point in space (see Table 1 for a list of notations). This one-dimensional (1D) notation is chosen for simplicity. In the usual two-dimensional (2D) case, x is used for, say, (x',y'), and space integrals appear as simple rather than double integrals. This lightens the equations without any loss of generality. The fish density $z(x)$, taken as a function of space, is a regionalized variable expressed, for instance, as the number of individuals (ind.) per unit surface area (e.g., ind.$\cdot$m^{-2}).

The covariogram (Matheron 1971) is defined by the space integral of the product of pairs of densities a given distance h apart:

$$(1) \qquad g(h) = \int z(x)z(x+h)\mathrm{d}x$$

In 2D, it is expressed as the squared number of individuals per unit surface area (e.g., ind.$^2\cdot$m^{-2}). The distance h is a vector distance with a modulus and a direction. When the covariogram is the same for all directions, it is said to be isotropic; otherwise, it is said to be anisotropic.

The total fish abundance Q is

$$(2) \qquad Q = \int z(x)\mathrm{d}x$$

Using the density relative to the total abundance leads to the relative covariogram (Bez and Rivoirard 2001)

$$(3) \qquad g_\mathrm{r}(h) = \frac{g(h)}{Q^2} = \frac{\int z(x)z(x+h)\mathrm{d}x}{\left(\int z(x)\mathrm{d}x\right)^2}$$

which will be used in the rest of the paper.

Properties and meanings of the relative covariogram

The relative covariogram globally decreases from its maximum value $g(0)$, taken as an index of aggregation (Bez and Rivoirard 2001), to 0 at long distances (Fig. 1). The distance at which the covariogram reaches zero (strictly or asymptotically) is called the range. It quantifies the maximal diameter of the population in the particular direction of concern. The range is therefore a geometrical property of the areal distribution of the population. The covariogram is isotropic in 2D for circular populations. This is often unrealistic in fisheries applications, and covariograms of fish densities will generally be anisotropic, although it is sometimes difficult to determine this anisotropy in practice.

The behaviour of the covariogram near the origin, that is, for small distances (h), is related to the spatial continuity of the fish density. When there is large local heterogeneity, there is large variation between neighbouring fish concentrations and thus a large decrease exists at the origin of the covariogram. In practice, this decrease is observed rather as a discontinuity owing to the spacing between data points. One can theoretically distinguish two reasons for local heterogeneity: the small-scale fish distribution itself and nonsystematic measurement errors. The latter, even though present in most cases, is often unknown, and splitting the discontinuity of the covariogram into terms for measurement errors and small-scale structures is impossible in practice. Therefore, a relative covariogram model can be written (Fig. 1):

$$(4) \qquad g_\mathrm{r}(h) = C_0 1_{h=0} + C_1 g_{\mathrm{r},1}(h)$$

where $1_{h=0}$ is the function equal to 1 for distance $h = 0$ and 0 otherwise, also called the nugget effect. The amplitudes (sills) of the nugget effect and of the continuous parts of the model are C_0 and C_1, respectively.

Global estimation coefficient of variation from strictly regular sampling

Following the 1D notation, the origin of the sampling grid (i.e., the starting point of a regular survey) is denoted x_0, and the grid mesh interval is denoted s. A sample point is then located at $x_0 + ks$, i.e., the origin plus an integer multiple of the grid mesh interval. The total fish abundance is estimated by the sum of the sample values times the surface of the grid mesh

$$(5) \qquad Q^* = s\sum_k z(x_0 + ks)$$

No probabilistic hypothesis has yet been made and the estimator is a deterministic quantity. Let us now assume that the location of the origin of the sampling grid is randomly located. It can therefore be interpreted as the outcome of a random variable x_0 with uniform distribution over the grid mesh. The estimator, now denoted $Q^*(X_0)$, becomes a random variable because of the randomness of the origin. Its bias is 0 because of the uniform distribution of X_0:

$$(6) \qquad E[Q^*(X_0)] = \int_s Q(x)\frac{\mathrm{d}x}{s}$$

$$= \int_s s\sum_k z(x+ks)\frac{\mathrm{d}x}{s}$$

$$= \sum_k \int_s z(x+ks)\mathrm{d}x$$

Table 1. List of symbols and variables used in the text.

Notation	Unit	Meaning
x	Degree or n.mi.	A point in space $x = x'$ in 1D $x = (x',y')$ in 2D $x = (x',y',t')$ in 3D, etc.
$z(x)$	**ind.·m^{-2}** (ind.·m^{-2}·day^{-1} or kg·m^{-2})	Fish density at x · regionalized variable
Q	**ind.** (ind.·day^{-1} or kg)	Total fish abundance
h	n.mi.	Vectoral distance
$g(h)$	**ind.^{2}·m^{-2}** (ind.^{2}·m^{-2}·day^{-2} or kg^2·m^{-2})	Covariogram
$g_r(h)$	n.mi.$^{-2}$	Relative covariogram
N_f	None	Number of functions in the covariogram model, excluding the nugget effect
C_0	n.mi.$^{-2}$	Nugget effect amplitude
$g_{r,1}(h)$	None	Relative covariogram excluding the nugget effect.
$g_{r,1,i}(h)$	None	Various components of $g_{r,1}(h)$ (nugget effect excluded)
C_1	n.mi.$^{-2}$	Amplitude of of $g_{r,1}(h)$
$C_{1,i}$	n.mi.$^{-2}$	Amplitudes of the various components of $g_{r,1}(h)$
$a_{1,i}$	n.mi.	Ranges of the various components of $g_{r,1}(h)$
$\mathrm{dir}_{1,i}$	Degree	Directions of anisotropy of the various components of $g_{r,1}(h)$
$\mathrm{ani}_{1,i}$	None	Coefficient of anisotropy of the various components of $g_{r,1}(h)$
x_0	Degree or n.mi.	Coordinates of the sampling grid origin
s	n.mi.^{2}	Grid mesh interval
k	None	Sampling index
N	None	Number of samples
X_0	Degree or n.mi.	Random variable grid origin (uniform over the grid mesh interval s)
$Q^*(X_0)$	**ind.** (ind·day^{-1} or kg)	Estimation of Q
σ_E^2	**ind.^{2}** (ind^2·day^{-2} or kg^2)	Estimation variance
$\mathrm{CV_E}$	None	Coefficient of variation for Q^*
s_k	n.mi.^{2}	Grid squares
X_k	Degree	Coordinates of random sample in each grid cells
A	n.mi.^{2}	Surface area occupied by the population.

Note: 1D, one dimension; 2D, two dimensions; 3D, three dimensions; ind., number of individuals; n.mi., nautical miles. Usual units are given in bold. Possible alternatives are given in parentheses.

Fig. 1. Definition of a relative covariogram model $g_r(h)$: nugget effect ($1_{h=0}$) with sill C_0 and continuous part ($g_{r,1}(h)$) with sill C_1 and range a_1.

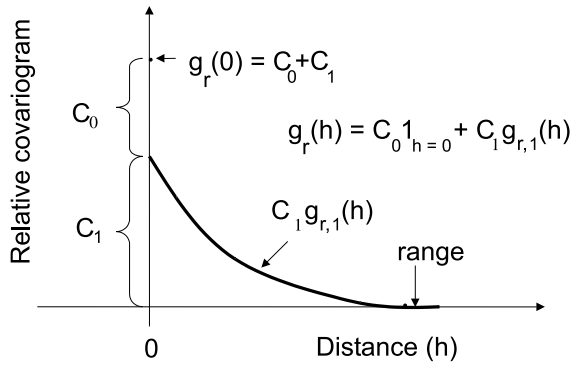

$$= \int z(x)\mathrm{d}x$$

$$= Q$$

After Matheron (1971), the estimation variance

$$\sigma_E^2 = \mathrm{var}(Q^*(X_0) - Q) \tag{7}$$

$$= E(Q^*(X_0) - Q)^2$$

can be expressed as the difference between the discrete and the exact integral of the covariogram. Using the relative covariogram leads to the estimation coefficient of variation ($\mathrm{CV_E}$):

$$\mathrm{CV_E} = \frac{\sigma_E}{Q^*} = \sqrt{s\sum_k g_r(ks) - \int g_r(h)\mathrm{d}h} \tag{8}$$

The smaller the grid mesh interval, the smaller the estimation CV. The difference between the discrete sum and the true integral also depends on the regularity of the covariogram and, more specifically, on its behaviour near the origin (e.g., the spatial regularity of the fish density). The estimation CV increases when moving from spatially regular to spatially irregular fish densities, that is, from covariogram with a parabolic to a discontinuous behaviour at the origin (Chilès and Delfiner 1999; Fig. 2). When a significant nugget effect exists, it explains nearly all of the estimation CV (Fig. 2), which can then be approximated by

$$\mathrm{CV_E} = \sqrt{sC_0} \tag{9}$$

Fig. 2. Global estimation coefficient of variation (CV) and behaviour of the relative covariogram near the origin. The estimation CV corresponds graphically to the difference between the solid and the shaded areas. It increases when the spatial local heterogeneity of the fish density, i.e., C_0, increases: (*a*) no nugget effect and parabolic behavior, very small estimation CV; (*b*) no nugget effect and linear behavior, small estimation CV; (*c*) reasonable nugget effect and linear behavior, large estimation CV; (*d*) large nugget effect and linear behavior, very large estimation CV.

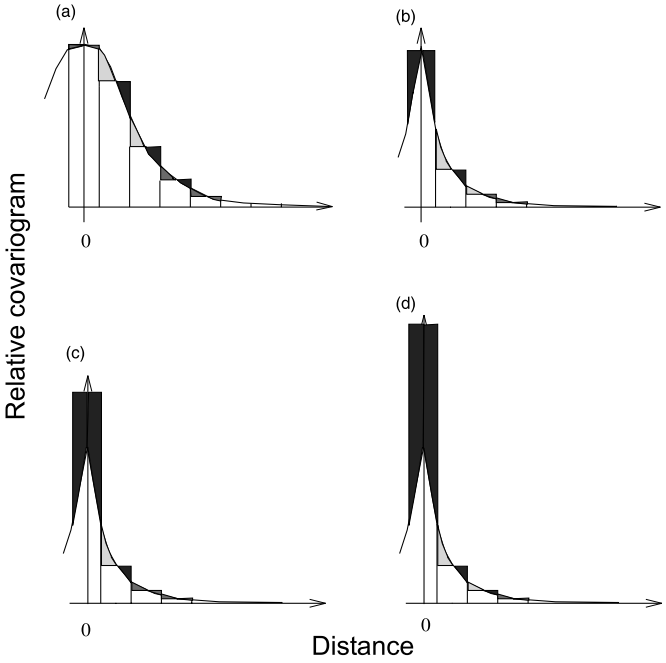

The bias refers to all estimations that would be computed if resampling were possible with many different grid origins. To avoid systematic errors over a series of annual surveys, one should change the origin of the grid from year to year. One alternative is to use a random stratified sampling.

Global estimation variance from random stratified sampling

A regular stratified sampling is one in which one sample is located at random in each cell of a regular grid and independently from the other cells. Strata are cells of the grid. Many surveys use this sampling design (e.g., the International Bottom Trawl Surveys in the North Sea (ICES 1997), the snow crab (*Chionoecetes opilio*) survey in Canada (Conan et al. 1988), and the Moroccan cephalopod surveys).

Using the 1D notation, each sample point X_k, $k \in [1,N]$ where N is the number of samples, is random uniform in its grid cell s_k. The estimator of the abundance is a random variable function of a set of identically and independently distributed random variables:

$$(10) \quad Q^*(\{X_k\}) = s\sum_k z(X_k)$$

Here again, the randomness concerns the sampling process and not the fish density. As X_k is random uniform over its grid cell s_k, the estimator is unbiased:

$$(11) \quad E[Q^*(\{X_k\})] = s\sum_k E[z(X_k)]$$

$$= s\sum_k \int_{s_k} z(x)\frac{\mathrm{d}x}{s}$$

$$= Q$$

Because of the independence of sample locations between grid cells, Matheron (1971) showed that the estimation variance only depends on the behaviour of the covariogram at distances smaller than the grid mesh size. The estimation CV is then

$$(12) \quad \mathrm{CV_E} = \sqrt{s(g_\mathrm{r}(0) - \overline{g_\mathrm{r}(s)})}$$

where $\overline{g(s)}$ is the mean value of the covariogram between two points x and y located independently in a grid cell s:

$$(13) \quad \overline{g_\mathrm{r}(s)} = \frac{1}{s^2}\int_s\int_s g_\mathrm{r}(x-y)\mathrm{d}x\,\mathrm{d}y$$

Note that this is different from the mean value of the covariogram for distances between 0 and s. With the generic form of covariogram given in eq. 4, $\mathrm{CV_E}$ simplifies to

$$(14) \quad \mathrm{CV_E} = \sqrt{sC_0 1_{h=0} + sC_1(g_{\mathrm{r},1}(0) - \overline{g_{\mathrm{r},1}(s)})}$$

Practical implementation

Covariogram estimation

With regular grids, which are preferred, the relative covariogram is estimated for any distance and direction in the grid. Most logical directions correspond to the two main directions of the grid where sampling density is highest, but all diagonal directions can be looked at. Following Matheron (1971), the relative covariogram for a distance equal to a multiple l number of grid intervals $l{\cdot}s$ is estimated by the sum of the products of pairs of densities separated by l grid nodes:

$$(15) \quad g_\mathrm{r}(ls) = \frac{\sum_k z(x_0 + ks)z(x_0 + ks + ls)}{s\left(\sum_k z(x_0 + ks)\right)^2}$$

This assumes that the fish density is zero beyond the sampling area.

For random stratified sampling, one can assume regularity and put actual distances into distance classes in accordance with the grid size or use one of the weighted procedures suggested by Bez et al. (1995).

Numerical layout and units

When computing the covariogram, fish density and grid mesh surface area should be expressed with compatible units. However, there are cases in which fish density is expressed in units that do not simplify with those of a surface area (i.e., $\mathrm{kg{\cdot}h^{-1}}$). A relative covariogram is expressed as the inverse of a surface area, whatever the units of the fish density. This makes it more practical to use than the covariogram, as one has simply to ensure consistency between distance units (x axis of the relative covariogram) and surface area units (y axis of the relative covariogram):

$$(16)\quad \text{units of } \left(\frac{g(h)}{Q^2}\right) = \frac{(\text{units of } z)^2 \times (\text{units of } s)}{((\text{units of } s) \times (\text{units of } z))^2} = \frac{1}{(\text{units of } s)}$$

Reference system

Computation of distances between points often requires the projection of data points in a Euclidean reference system. Regular sampling might be no longer regular after projection because of some cosine operations. The method is then appropriate for samplings that are regular in the projected space.

Covariogram fitting

The model must be symmetrical, bounded, and positive or null when the fish density is positive or null and ensure that the estimation variance is always positive (or null). Not all mathematical functions (in particular, polynomial functions) fulfil these requirements. To prevent inconsistencies in the model, a set of allowable functions has been defined (e.g., Chilès and Delfiner 1999). Most of these functions are defined by only one parameter controlling the range (further denoted a) of the function, i.e., the distances beyond which the function is either null or below 5% of the value at the origin.

The anisotropy is often modeled by two parameters (Journel and Huijbregts 1978): the direction (dir) in which the range is given and the coefficient (ani) by which the range has to be divided to get the range in the orthogonal direction. The range for an intermediate direction corresponds to the radius of the ellipse defined by the maximum and minimum range in the appropriate directions (Fig. 3). When a covariogram is made of several functions, the anisotropy of each function can be different from that of the others.

The continuous part of a model is therefore a combination of N_f allowable functions defined by four N_f parameters: N_f ranges, N_f amplitudes, N_f directions of anisotropy, and N_f coefficients of anisotropy:

$$(17)\quad g_r(h) = C_0 1_{h=0} + \sum_{i=1}^{N_f} C_{1,i} g_{r,1,i}(h, a_{1,i}, \text{dir}_{1,i}, \text{ani}_{1,i})$$

Once a set of N_f functions is chosen, fitting consists of estimating the four N_f parameters and C_0. This can be done using any kind of parametric regression method. In the present study, the anisotropy parameters are set manually, whereas the other ones are estimated by the least squares method. Thereafter, parameter C_0 is deduced by the difference between the experimental value at the origin and $C_1 g_{r,1}(0)$. A graphical control of the fit is systematic to avoid overly optimistic fittings.

Applications

Eggs surveys in the northeast Atlantic

Since 1977, international triennial eggs surveys, coordinated by ICES, have been carried out to assess mackerel (*Scomber scombrus*) and horse mackerel (*Trachurus trachurus*) stock sizes (Lockwood et al. 1981; ICES 1996). The sampling tries to encompass the space (Bay of Biscay, Celtic Sea, and West of Ireland) and time (February–July) of the whole spawning season, with four or five sampling periods, depending on the year. The present study deals with the production of stage I mackerel eggs during sampling period 2 of 1989.

Fig. 3. Model of the anisotropy. The ellipse represents the value of the range for all directions. The example corresponds to the exponential part of the relative covariogram model of mackerel eggs, i.e., a covariogram with range 390 nautical miles (n.mi.) with a geometrical anisotropy of direction –58° and coefficient 3.5.

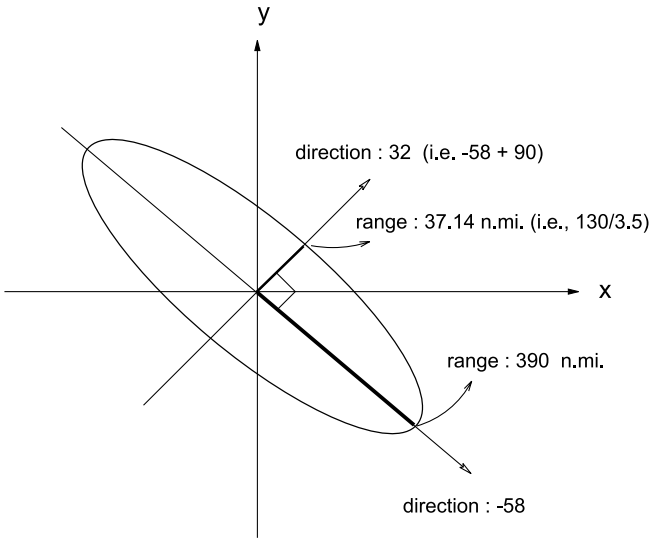

The sampling follows a regular grid of 0.5° of longitude × 0.5° of latitude. The origin of the sampling grid was arbitrarily located the first time (1977) and not randomized since. In some grid cells, duplicate samples are made and averaged prior to the estimation.

Samples were collected by oblique hauls (with Bongo or Gulf III nets with 500 μm mesh) from the surface to a certain depth and then back to the surface (Lockwood et al. 1981). Maximum sampling depth is either the bottom, or 200 m deep, or 20 m below the thermocline when this exceeds 2.5°C per 10 m depth. Following the standard procedure established by the ICES Working Group on Mackerel and Horse Mackerel Egg Surveys, eggs were staged and counted. Knowing the water temperature at each sample point and the duration of each developmental stage as a function of the temperature (Lockwood et al. 1981), a daily production of stage I eggs was provided for each sample location (Fig. 4). These were expressed as the number of eggs per day and square metre (ind.·m^{-2}·day^{-1}).

Decimal latitudes have been multiplied by 60 and decimal longitudes by 60 times the cosine of the mean latitude of the sample points (51°00′N). The grid is then still regular after projection, and the distances and the grid mesh surface area are expressed in nautical miles (n.mi., 1 n.mi. = 1852 m):

$$(18)\quad s = 0.5 \times 0.5 \times 60 \times 60 \times \cos(51) = 566 \text{ n.mi.}^2$$

The estimated daily production of eggs over the entire sampling field is

$$(19)\quad Q^* = s \cdot 1852^2 \sum_k z_k = 2.33 \times 10^{13} \text{ ind.·day}^{-1}$$

where z_k is the sample values at grid cell k (1852^2 ensures consistent units between s and z_k. The relative covariogram

Fig. 4. Proportional representation of the daily production of stage I mackerel (*Scomber scombrus*) eggs (ind.·m^{-2}·day^{-1}) of the second sampling period of the 1989 survey. Squares have a surface proportional to the data. Crosses represent zero data. The 200-m isobath is shown (dotted line). Inset of Europe shows sampling area in the northeast Atlantic.

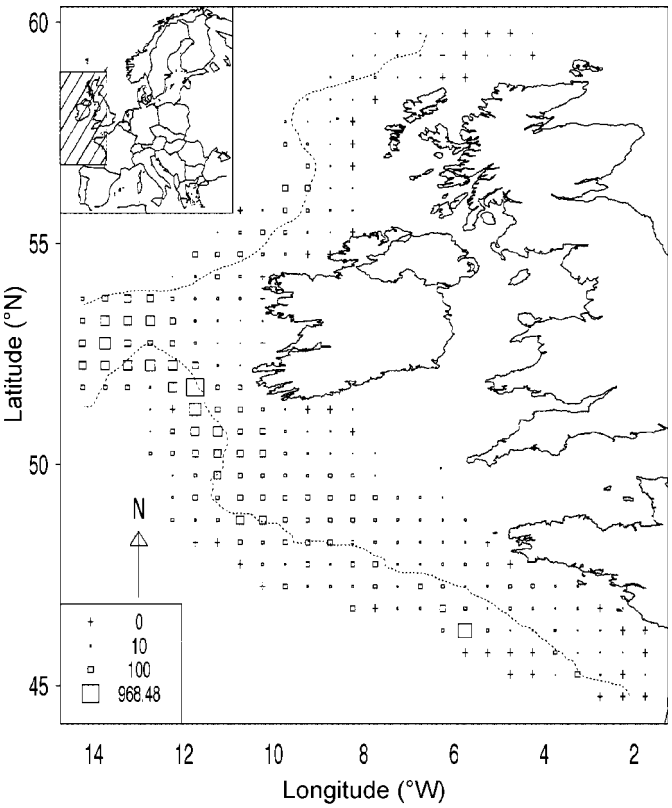

has been computed for four different directions: the two main directions of the grid (east–west and north–south) and the two bisectors (Fig. 5). The directions are given in trigonometric angles: 0 for the east–west direction and 90 for the north–south one. The model fit to the experimental data consists of a nugget effect explaining one-third of the overall spatial structure and an anisotropic exponential function (see Table 2 for model parameters). This leads to an estimation CV of 8.4%. The approximation given in eq. 8 gives a CV equal to 7.7%.

In this example (stage I mackerel egg production rate, 2nd sampling period, 1989), even though one-third of the egg spatial structure is due to scales smaller than the intersample distance and to random measurement errors, the CV of the global estimation is low. This indicates that, in this case, despite the importance of small-scale variability, the spatial coverage of the sampling is fine enough to ensure confidence in the order of magnitude of the overall egg production estimate. The uncertainties associated with the species determination of the eggs and their staging are not taken into account in the above coefficient of variation.

Cephalopod surveys in Morocco

Since 1980, trawl surveys have been performed by the National Institute of Fisheries Research (INRH) of Morocco to study the Moroccan stocks of octopus (*Octopus vulgaris*) in Atlantic waters. A random stratified survey takes place in spring and autumn, the reproductive and recruitment periods for octopus in this region. A grid with cells of 11 n.mi. × 11 n.mi. (Fig. 6) covers the entire population, seeking an optimal number of samples given the time allocated to the survey. Here we present data for the October 1998 survey (N = 106 samples).

Samples were collected using a Spanish bottom trawl adapted for cephalopods. A differential geographical positioning system (GPS) and a sonar system were used to monitor the swept areas so that sample values were expressed as metric tonnes of octopus per square meter (t·m^{-2}). In October 1998, the bulk of the population was concentrated in a small coastal area around the latitude 24°00′N (Fig. 6). Zeroes were obtained at the northern and western borders of the sampling grid, indicating that sampling exceeded the population distribution in these directions. Southwards, the survey is limited by the national border between Morocco and Mauritania, which does not correspond to a natural border of octopus (Bravo de Laguna and Balguerias 1993; FAO 1997). As the objective of the study is to estimate the abundance of octopus in the Moroccan waters and because we lack data beyond this border, we assume that the densities are null beyond the survey area.

Based on the work of Bez et al. (1995) for irregular sampling, the relative covariogram has been estimated for directions 15°, 60°, 105°, and 150° (Fig. 7). A model with a nugget effect and two anisotropic spherical functions has been fit (see Table 2 for model parameters).

The estimated total abundance is 23 263 t with an estimation CV of 17%. The ratio $C_0/C_0 + C_1$ is smaller than for the mackerel egg example (20 vs. 30%). However, the estimation CV is larger because the relative covariogram, and in particular C_0, for the octopus data is 10 times larger than for mackerel data, indicating that there is more unexplained variability in octopus.

Discussion

Model characteristic, sensitivity, and robustness

Covariogram models are defined by a relatively low number of parameters: five for the present mackerel egg study and nine for the octopus estimation, including the anisotropic parameters. The most important parameter for the estimation variance is the parameter C_0, the estimation of which is deduced from the behaviour of the covariogram at distances smaller than the grid mesh, for which we have no observation. The behaviour of the structure from the first distance lag to 0 is extrapolated on the basis of the behaviour of the entire covariogram and of the physical and mathematical properties of covariograms. These properties act as constraints and provide more confidence in the behaviour of the covariogram near the origin. We considered several different forms of covariogram models to evaluate the sensitivity of the results to the model characteristics. In the first case study, automatic fitting is possible with either one spherical and two spherical models. This leads to nugget effects of 14 and 12 × 10^{-6} n.mi.$^{-2}$, respectively, whereas the goodness of fit (Rivoirard et al. 2000) is the same. The coefficient of variation (eq. 8) associated with the model with the largest nug-

Table 2. Relative covariogram model parameters.

	Nugget effect	Amplitude of the continuous part	Proportion of nugget	First function					Second function					
Parameter	C_0	C_1	$\frac{C_0}{C_0 + C_1}$	$g_{r,1,1}(h)$	$C_{1,1}$	$a_{1,1}$	$\mathrm{dir}_{1,1}$	$\mathrm{ani}_{1,1}$	$g_{r,1,2}(h)$	$C_{1,2}$	$a_{1,2}$	$\mathrm{dir}_{1,2}$	$\mathrm{ani}_{1,2}$
Units	10^{-6} n.mi.$^{-2}$	10^{-6} n.mi.$^{-2}$	%		10^{-6} n.mi.$^{-2}$	n.mi.	Degree			10^{-6} n.mi.$^{-2}$	n.mi.	Degree	
Mackerel eggs	10.5	25.3	29	expo	25.3	390	–58	3.5	—	—	—	—	—
Octopus	120	490	20	Spherical	340	50	60	2	Spherical	150	110	60	3

Note: Two functions have been used. The exponential model defined by $\mathrm{expo}(h,a) = e^{-\frac{|h|}{a}}$ and the so-called spherical model defined by $\mathrm{spherical}(h,a) = \begin{cases} 1 - \frac{3|h|}{2a} + \frac{|h|^3}{2a^3} & \text{if } h \le a \\ 0 & \text{if } h > a \end{cases}$

get effect is 9.2%. We found 8.4% using an exponential model. In the second case study, using only one spherical model leads to a larger nugget effect than that of the chosen model (190×10^{-6} n.mi.$^{-2}$) but decreases the quality of the fit. Exponential models are rejected by the automatic fitting procedure. The coefficient of variation (eq. 12) derived from this new model is 18.7%, whereas we found 17%.

According to the particular locations of the data points of a given survey, the experimental covariogram is expected to depart from the true but unknown relative covariogram and to fluctuate around it from survey to survey. Thus, global estimations and their CV_E depend on the particular locations of the data points. In a simulation exercise, which is the only way to work on a known system, covariogram fluctuations owing to sampling appear to be maximal at the origin and decrease as the distance h increases (A. Faraj, Institut National de Recherche, 2 rue de Tiznit, Casablanca, Maroc, unpublished data). This reduces the confidence that one has in a single result. Series of surveys are helpful in this regard.

Comparison with other techniques

Quality of an estimator

Within a given probabilistic framework, the quality of an estimator is quantified by its bias, its convergence, and its precision (Saporta 1990). The bias, which is expected to be null, is the error made on average over several estimations made in the same conditions. The convergence states that when the sample size increases, the estimate must get closer and closer to the true unknown value or, equivalently, that the estimation variance must get closer and closer to zero. The precision is often quantified by the estimation variance, and one would favour estimators with low coefficient of variation. However, the sole use of these three quality parameters could be misleading when choosing between estimators that are not based on the same assumptions. The use of the median to estimate the mean of a variable is a good example of this difficulty. The median is known to be less sensitive to extreme values (i.e., outliers) than the arithmetic mean. However, the convergence of the median only holds if the distribution of the variable is symetrical, whereas the arithmetic mean converges to the true mean whatever the distribution. Therefore, the usefulness of the median depends on a new assumption, which makes the entire estimation process less robust, that is, more sensitive to possible discrepancy between the data and the model assumptions.

Therefore, in addition to the bias, the convergence, and the estimation variance, when choosing, for instance, between design-based and model-based estimators, one must then consider the number and the falsifiability of the hypotheses of the respective approaches. The falsifiability of a hypothesis is our capacity to control in practice its adequacy to field data.

Design-based vs. model-based geostatistical approaches

In the transitive approach, which is a design-based approach, the major assumption concerns the randomness of either the origin of the sampling grid or the location of sampling points in the grid cells. Such assumptions are easy to control in practice. This differs fundamentally with the classical model-based geostatistical approach in which the sto-

Fig. 5. Experimental and modeled relative covariogram for mackerel (*Scomber scombrus*) eggs (ICES (International Council for the Exploration of the Sea) triennial survey 1989 2-day sampling period) in four irregular directions given in trigonometric angles: 0°, open circles, continuous line; 58°, open squares, dotted line; 90°, solid circles, short-dashed line; 122°, solid squares, long-dashed line. Distance is in nautical miles (n.mi.), relative covariogram, $\times 10^{-6}$ n.mi.$^{-2}$.

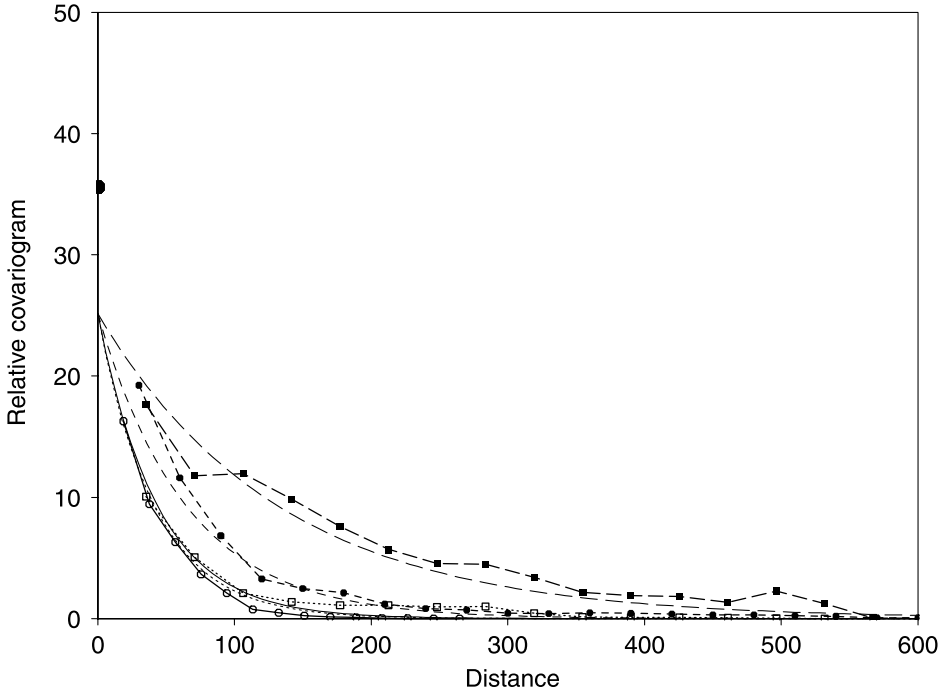

chastic part of the model and thus the constituent hypotheses concern the density itself considered as a realization of a random function (Rivoirard et al. 2000). Assumptions that concern the stationarity of some aspects of the process (e.g., the expected value and the variance for simple cases) are much more difficult to control in practice.

Area-based vs. area-free approaches

All samples, including the zero data, are considered. Zero data do not influence the results because the method refers to spatial integrals and because sums are unaffected by the addition of zero data. The method does not require the delineation of the transition between inside and outside the population. This explains the term transitive and makes the technique area-free. Still, the zeroes are not ignored and represent crucial information. Their presence tells us whether or not the whole population has been sampled and, thus, allows for the meaningful use of the method. In practice, zeroes must have been observed or unsampled areas can be assumed empty. In the first study case, it is possible that parts of the egg distribution are missing, as indicated by the large values at the western ends of transects around 53°00′N.

Any method based on averages (intrinsic geostatistics, spectral analyses, usual statistics, generalized linear or additive models, etc.) refers to a field that has to be defined before estimation. They are area-based. After a polygon is defined, the use, for instance, of the classical estimation variance ($\sigma^2_{iid} = s^2/N$) based on the assumption that samples are independent and identically distributed, leads to coefficients of variation of 12.5 and 24.6% for the two case studies, respectively. In these cases, taking into account the spatial structure improves the coefficient of variation.

The definition of the population boundary is often a difficult and subjective step in open marine systems mainly because of the zero data. The transitive method allows for the computation of the variance of the error made when estimating the boundary somewhere between zero and nonzero observations (Matheron 1971). This geometrical variance (not presented here) can be added to the estimation variance of the abundance but is often negligible.

Spatial versus spatiotemporal approaches

The transitive approach, like most survey data analyses, implicitly assumes that data have been taken at the same time, which is never true. In some cases (e.g., migrating pelagic fish), bias may be expected if the probability of sampling individuals twice or to miss some parts of the stock is large. However, in other cases, the behaviour of the target animals during the survey is such that the global estimate can be still considered reliable. For egg production, the survey lasted 22 days, whereas the spawning season, during which the spawning activity fluctuates slowly, lasts approximately 4 months. Thus, even though the first and last observations are about 3 weeks apart, they adequately represent the overall level of spawning at the time of sampling in the spawning process. In the second case, octopus are sedentary and quite immobile. Thus, the time elapsed during the survey (1 month) matters little. However, approaches exist that address some spatiotemporal issues.

Helbig and Pepin (1998), for instance, developed a biophysical model to distinguish between natural and physical (mainly advection) causes when estimating plankton mortality over a series of surveys. Advection and, to a lesser degree, diffusion are taken into account mainly to compare

Fig. 6. Proportional representation of octopus (*Octopus vulgaris*) densities ($t \cdot m^{-2}$) as observed during the Moroccan survey in October 1998. Dashed lines represent the grid used for implementing the samples (one sample located at random in each cell of the grid given that no rocky area is encountered). Squares have a surface proportional to the data values. Crosses represent zero data. Inset of Africa shows Morroccan survey area.

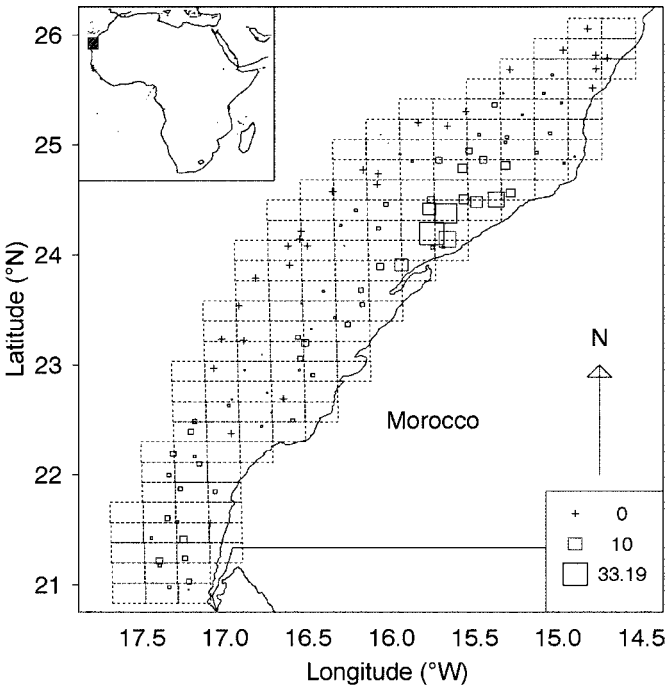

biomass between surveys, not to estimate the amount of plankton at a given time from a nonsynoptic survey. As for universal kriging (Matheron 1971), Helbig and Pepin assumed that densities have a spatiotemporal trend and that the residuals can be modeled by a spatiotemporal stationary random function (the time trend is small at the survey scale). This framework can be regarded as being more flexible and thus more adaptable to practical cases than the transitive approach. The counterpart of this flexibility is that it is based on more numerous and stronger hypotheses and on more parameters. In particular, if the number of observations is low compared with the population area and the heterogeneity of the variable, the estimation of a trend, a covariance, or a spectral function may not be objective and realistic. This was regarded to be the case for egg distributions in the northeast Atlantic, leading precisely to the use of a transitive approach (Bez and Rivoirard 2001). The tradeoff between bias and variance when defining the trend may also lead to overly optimistic estimates if the trend is not supported by enough observation (Matheron 1971).

The potential of generalized additive models (GAM) has also been evaluated for application to spatiotemporal observations (Augustin et al. 1998). These regression techniques generally enlarge the number of explanatory variables that are taken into account and then potentially have a stronger descriptive power than simpler methods. Here again, the parameterization of the model can become a weakness if the quality and the number of data do not allow a realistic enough control of the model assumptions. Augustin et al. (1998) have modeled egg density survey data as a smooth function of space, time, and oceanographic variables. They used the model to provide a global estimate of egg production and suggested a bootstrap procedure to compute an estimation variance. However, even with exhaustive information, egg density could be modeled by a set of smooth functions having residuals. The bootstrap procedure based on these residuals will then provide, contrary to the convergence property, a positive estimation variance.

Taking time into account aims at increasing the adequacy between field data and the model. However, using a 3D model instead of a 2D one may lead, contrary to expectation, to an increase of estimation variance because the same amount of information is used to fit a more complex model. At best, a regular space–time distribution of the data allows us to describe one particular direction of the 3D space. Working on day–night effect, Rivoirard and Wieland (2001) observed that although the estimated abundance was not significantly changed when using a spatiotemporal model, estimation variances were larger.

Sampling limitations

As mentioned in Introduction, the transitive method is an appropriate technique for regular sampling schemes. There are two fundamental reasons for that. First, realistic estimates of the covariogram are only available for regular samplings where each observation gets the same area of influence s. Let us consider the first and the second point of any pair of observations ($z(x_0 + ks)$, $z(x_0 + ks + ls)$) used for the estimation of the covariogram at distance $l \cdot s$ (eq. 15). When the first point covers its surface of influence, which amounts to considering the true integral of the covariogram (eq. 3), so does the second one. Therefore, weighting their product by s allows an effective estimate of the covariogram. In an irregular sampling, the second point would have a different surface of influence. Weighting by s no longer represents the number of pairs in the true integral and a complex weighting procedure has to be used (Bez et al. 1995). The second reason is that estimation variance (eq. 8) is based on the fact that combining all possible outcomes of the random starting point of a sampling grid and the grid nodes amounts to covering the space entirely. This is no longer true for irregular samplings.

Measurement errors

Measurement error is often modeled by a random variable with a zero mean and a given variance, but without any autocorrelation and any correlation with the fish density itself. In this case, we no longer observe the true density $z(x)$, but $y(x) = z(x) + w(x)$, where $w(x)$ is the random white noise. Given that the mean of $w(x)$ on the study field of surface A is 0 and its variance is σ_w^2, one can show that only the nugget effect is affected by the measurement errors:

$$g_r^y(h) = A\sigma_w^2 1_{h=0} + g_r^z(h) \tag{20}$$

$$= C_0' 1_{h=0} + C_1 g_{r,1}(h)$$

and that the estimation CV increases by $\sqrt{sA\sigma_w^2}$. When measurement error increases, C_0 and CV_E increase accordingly.

Fig. 7. Experimental and modeled relative covariogram for octopus (*Octopus vulgaris*) computed in four regular directions given in trigonometric angles: 15°, open circles, continuous line; 60°, open squares, dotted line; 105°, solid circles, short-dashed line; 150°, solid squares, long-dashed line. Distance given in nautical miles (n.mi.), relative covariogram, × 10^{-6} n.mi.$^{-2}$.

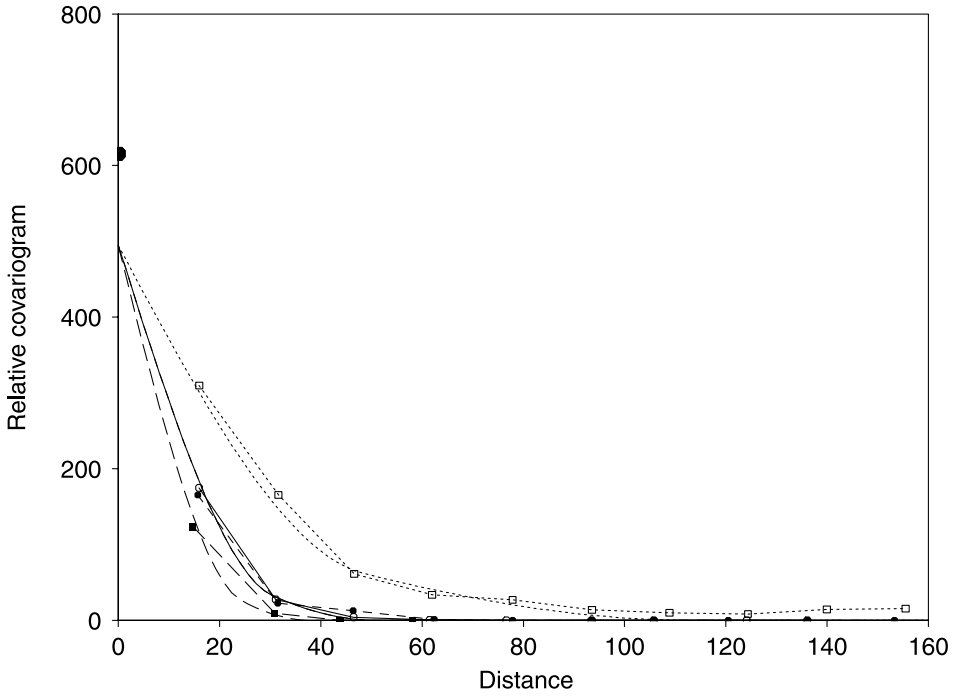

In conclusion, the transitive approach, a spatially explicit technique, allows for a design-based global estimation of abundance with an estimation variance for regular or regular stratified sampling. This theory makes relatively few assumptions (randomness of either the origin of the sampling grid or the location of data points in grid cells) that are easily controlled in practice (i.e., falsifiable). Together with the low number of parameters to be estimated, this ensures robust results. However, as it is designed strictly for spatial applications, it assumes that all observations are synoptic.

Acknowledgements

I am very grateful to colleagues who kindly provided data: the Institut National de Recherche Halieutique of Casablanca (Morocco) and all members of the International Council for the Exploration of the Sea (ICES) Working Group on Mackerel and Horse Mackerel Egg Surveys who perform the enormous sea and laboratory work required to update the egg database every 3 years. This work was conducted during EU Project 97/017 (acronym INDICES) aimed at estimating ichthyoplankton indices of abundance of spring-spawning commercial fish populations in western European waters. I am also very grateful to D. Checkley for his numerous and helpful comments on the manuscript and to anonymous reviewers who contributed to the Discussion section.

References

Augustin, N.H., Borchers, D.L., Clarke, E.D., Buckland, S.T., and Walsh, M. 1998. Spatiotemporal modelling for the annual egg production method of stock assessment using generalized additive models. Can. J. Fish. Aquat. Sci. **55**: 2608–2621.

Bez, N., and Rivoirard, J. 2001. Transitive geostatistics to characterize spatial aggregations with diffuse limits: an application on mackerel ichtyoplankton. Fish. Res. **50**: 41–58.

Bez, N., Rivoirard, J., and Poulard, J.C. 1995. Approche transitive et densités de poissons. Compte-rendu des journées de Géostatistique, 15–16 juin 1995, Fontainebleau, France. Cah. Géostat. **5**: 161–177.

Bravo de Laguna, J., and Balguerias, E. 1993. La pesqueria sahariana de cefalopodos : una breve revision. Bol. Inst. Esp. Oceanogr. **9**: 203–213.

Chilès, J.P., and Delfiner, P. 1999. Geostatistics, modeling spatial uncertainty. John Wiley and Sons, New York.

Cochran, W.G. 1977. Sampling techniques. John Wiley and Sons, New York.

Conan, G.Y., Moriyasu, M., Wade, E., and Comeau, M. 1988. Assessment and spatial distribution surveys of snow crab stocks by geostatistics. ICES CM 1988/K:10.

Cressie, N.A.C. 1991. Statistics for spatial data. John Wiley and Sons, New York.

Food and Agriculture Organisation (FAO). 1997. Rapport du groupe de travail ad hoc sur les céphalopodes. COPACE/PACE Ser. 97/63, FAO, Rome.

Helbig, J.A., and Pepin, P. 1998. Partitioning the influence of physical processes on the estimation of ichthyoplankton mortality rates. Can. J. Fish. Aquat. Sci. **55**: 2189–2205.

International Council for the Exploration of the Sea (ICES). 1996. Report of the Working Group on Mackerel and Horse Mackerel Egg Surveys. ICES CM 1996/H:2.

International Council for the Exploration of the Sea (ICES). 1997. Report of the International Bottom Trawl Survey Working Group. ICES CM 1997/H:6.

Journel, A.G., and Huijbregts, C.J. 1978. Mining geostatistics. Academic Press, London.

Lockwood, S.J., Nichols, J.H., and Dawson, W.A. 1981. The estimation of a mackerel (*Scomber scombrus* L.) spawning stock size by plankton survey. J. Plankton Res. **3**(2): 217–233.

Matheron, G. 1971. The theory of regionalized variables and its applications. Les Cahiers du Centre de Morphologie Mathématique No. 5.

Petitgas, P. 1993. Geostatistics for fish stock assessments: a review and an acoustic application. ICES J. Mar. Sci. **50**: 285–298.

Petitgas, P. 2001. Geostatistics in fisheries survey design and stock assessment: models, variances and applications. Fish Fish. Ser. **2**: 231–249.

Rivoirard, J., and Wieland, K. 2001. Correcting for the effect of daylight in abundance estimation of juvenile haddock (*Melanogrammus aeglefinus*) in the North Sea: an application of kriging with external drift. ICES J. Mar. Sci. **58**: 1272–1285.

Rivoirard, J., Simmonds, J., Foote, K., Fernandes, P., and Bez, N. 2000. Geostatistics for estimating fish abundance. Blackwell Sciences, Oxford.

Saporta, G. 1990. Probabilités, analyse des données et statistique. Technip, Paris.

Simmonds, J., and Fryer, R.J. 1996. Which are better, random or systematic acoustic surveys? A simulation using North Sea herring as an example. ICES J. Mar. Sci. **53**: 39–50.